

2nd International Conference on Sustainable Materials Processing and Manufacturing
(SMPM 2019)

Air pollution assessment: a preliminary study towards citing industry

Emetere M.E.^{a,c*}, Okoro E.E.^b, Adeyemi G.A.^d and Sanni S.E.^e

^a*Department of Physics, Covenant University Canaan land, P.M.B 1023, Ota, Nigeria.*

^b*Department of Petroleum Engineering, Covenant University Canaan land, P.M.B 1023, Ota, Nigeria*

^c*Department of Mechanical Engineering Science, University of Johannesburg, South Africa.*

^d*Department of Civil Engineering, Covenant University Canaan land, P.M.B 1023, Ota, Nigeria*

^e*Department of Chemical Engineering, Covenant University Canaan land, P.M.B 1023, Ota, Nigeria*

Abstract

The spate of increased air pollution in the study area is a source of concern. In this research, we examine the spatial distribution of atmospheric aerosol and its danger to the life form that resides therein. Fifteen years primary (aerosol optical depth) dataset was obtained from the Multi-angle Imaging Spectro-Radiometer (MISR). The secondary datasets that was generated from the primary data were aerosol loading, particles sizes, Angstrom parameter and the statistics of the primary dataset. It was observed that if not controlled, the life form in the research area may be under unimaginable danger in the near future. Hence, industrialization projects would require the dataset for environmental assessment before citing industry in the geographical area.

© 2019 The Authors. Published by Elsevier B.V.

Peer-review under responsibility of the organizing committee of SMPM 2019.

Keywords: air pollution, aerosol, Damaturu, Nigeria, model

1. Introduction

The One of the known methods for examining the level of pollution over an area is the aerosol optical depth (AOD). Optical properties of aerosol particles have severe influence over the local radiative forcing and radiation balance of the earth. The interaction between aerosol and solar radiation can be described by its optical

* Corresponding Author
Email: emetere@yahoo.com

properties. The optical parameters used to describe the aerosol-solar radiation are the extinction and scattering coefficients, the aerosol depth and the single-scattering phase. These parameters are wavelength dependent. The aerosol optical properties are majorly described by the aerosol optical depth (at 500 nm wavelength) and the Angstrom exponent. The aerosol optical depth can be defined as the negative natural logarithm of the fraction of solar radiation that is not scattered or absorbed on a path by aerosol particles. Angstrom exponent describes the dependency of the aerosol optical thickness, or aerosol extinction coefficient on wavelength.

In recent time, the aerosols loading of over fifty towns and cities across West Africa using basically the optical properties (Emetere, 2006). It was observed that the West Africa climate system was very unique and no single model could capture the aerosols loading of more than three towns or cities in West Africa. Based on the above, the West African regional scale dispersion model (WASDM) emerged as a regional aerosol model. WASDM have been used to successfully described the relationship between atmospheric aerosols and the West African climate system. The model was validated by the aerosols loading of over fifty towns and cities in West Africa ((Emetere et al. 2015, Emetere 2016a).

Yu and Xu (1987) worked on the regional and total deposition of 200 nm particles in the lungs of children and adult. It was observed that the total deposition in the tracheo-bronchial has risen by a factor of 20% in children relative to adults. This ascertainment was experimentally validated by Becquemin et al., (1990) and Schiller-Scotland et al, 1992). Hence, the focus of this research is to know the susceptibility of life-form (in the research area) to respiratory disfunction through the application of remote sensing techniques and proven mathematical models.

2. Materials and Methods

Damaturu is located on latitude 11.7470° N and longitude 11.9662° E, as shown on the map (Figure 1). The primary data was obtained from Multi-angle Imaging Spectro-Radiometer (MISR). The aerosol retention and loading were obtained using the West African regional scale dispersion model (WASDM) from the AOD dataset (Figures 2 and 3). The West African regional scale dispersion model (WASDM) for calculating aerosol loading over a region is given as (Emetere, 2016b):

$$\psi(\lambda) = a_1^2 \cos\left(\frac{n_1 \pi \tau(\lambda)}{2} x\right) \cos\left(\frac{n_1 \pi \tau(\lambda)}{2} y\right) + \dots \dots a_n^2 \cos\left(\frac{n_n \pi \tau(\lambda)}{2} x\right) \cos\left(\frac{n_n \pi \tau(\lambda)}{2} y\right) \quad (1)$$

a is atmospheric constant gotten from the fifteen years aerosol optical depth (AOD) dataset from MISR, n is the tuning constant, $\tau(\lambda)$ is the AOD of the area and $\psi(\lambda)$ is the aerosol loading.

The digital voltage and Angstrom parameters of the study area can be obtained from equation (2) and (3) respectively.

$$I(555) = \frac{I_0(555)}{R^2} \exp(m * \tau(555)) \quad (2)$$

where I is the solar radiance over the SPM detector at wavelength $\lambda = 555$ nm, I_0 is the is a measure of solar radiation behind the atmosphere, R is the mean Earth-Sun distance in Astronomical Units, τ is the total optical depth (in this case, the average of the each month is referred to as the total AOD, and m is the optical air mass.

$$\alpha = -\frac{d \ln(\tau)}{d \ln(\lambda)} \quad (3)$$

where α is the Angstrom parameter, τ is the aerosol optical depth, and λ is the wavelength. The radius of the particles for atmospheric aerosol and back-envelope was calculated using proposals by Kokhanovsky et al [2]. The analysis of equations (1-3) was done using the C++ codes, surfer software and excel.

The aerosols deposition into the human lungs (Figure 2) has been modelled as documented in Martonen and Zhang (1992) and Varghese and Gangamma (2006).

$$\eta = (1 - \exp(-39.9Q^{0.14}D^{0.599})) + (1 + \exp(12.39 - 2.92\log(\rho D_p^2 Q)))^{-1} \quad (4)$$

where η is the deposition efficiency, Q volumetric flow rate, D is the diffusion coefficient of the particle, ρ is the particle density and D_p is the particle diameter.



Figure 1: Google map over Damaturu

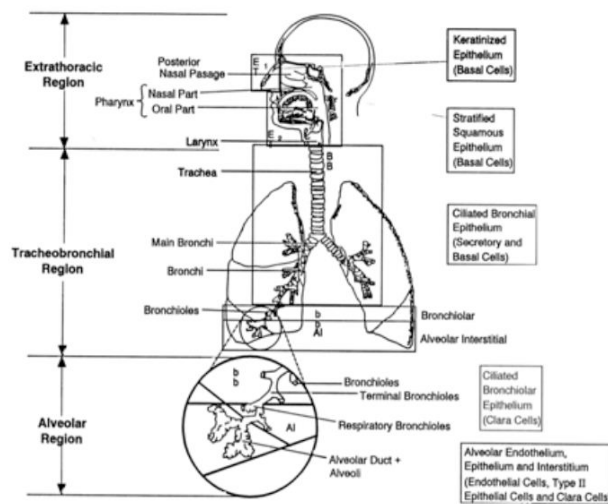


Figure 2: The respiratory component of the human being

3. Results and Discussion

The spatial distribution of the aerosol optical depth (AOD), aerosol retention (AR) and aerosol size distribution (ASD) is presented in Figure 3, Figure 4 and Figure 5 respectively. The concentration of the aerosol

optical depth can be found on the north-east of the research site. However, it is unclear if the AOD will spread to other parts of the area (Figure 3). This aspect is not within the scope of this research. The south west of the city have appreciable concentration. Hence, may infer that this event is caused by the north east winds (Emeteri, 2016b).

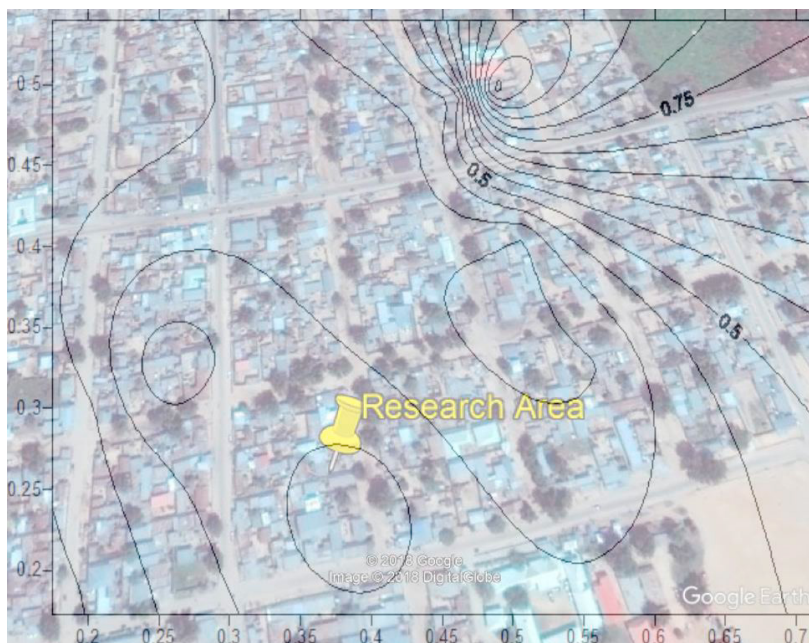


Figure 3: AOD distribution over Damaturu



Figure 4: Aerosol retention distribution over Damaturu



Figure 5: Aerosol size distribution distribution over Damaturu

The AR concentration is highest towards the south-west of the city (Figure 4). The lower concentration resides in the north-east of the city. The ASD replicates the same event as AOD (Figure 5). This means that the region of high concentration ASD may have low concentration AR. Table 1A-C presents the AR for over fourteen years. It can be inferred that the values of the AR fluctuates on yearly basis. This assertion is supported by Figure 6 below. However, it is observed that the AR is more active between June and December. In this period of the year, the influence of Sahara dust (Emetere 2016) is more prominent. The angstrom parameter is shown in Table 2. Like the aerosol loading and retestion, angstrom term fluctuates also. However, the documented values is important for the classification of the type of atmospheric aerosol. The value of the angstrom signifies that the aerosols over the city originates from dust and bush burning. For example, the north-east region (Figures 3-5) is the agarian region of the city. Hence, the life form is exposed to diverse kind of respiratory diseases as shown in Figure 7 where the maximum deposition efficiency in the human lungs is 95.62%. It is observed that the AR and ASD are directly proportional as presented in Figure 8. The statistics of the AOD is presented in Table 4. The year 2006 had the highest AOD. By inference, the AR will be lower spatially where the deposition efficiency (DE) will be high.

Table 1: Aerosol loading over Damaturu

Month	2000	2001	2002	2003	2004	2005	2006	2007	2008	2009	2010	2011	2012
Jan	0944	0922	0832	0904	0873	0866	0908	0873	0793	0850	0920	0880	0800
Feb	0944	0746	0889	0818	0811	0828	0793	0851	0759	0860	0882	0850	0780
Mar	0848	0843	0565	0798	0778	0714	0736	0795	0796	0785	0779	0855	0769
Apr	0857	0845	0855	0820	0824	0732	0821	0641	0794	0748	0760	0765	0765
May	0871	0826	0843	0849	0848	0906	0850	0817	0882	0830	0754	0764	0805
Jun	0819	0900	0895	0755	0846	0899	0890	0907	0870	0895	0863	0887	0809
Jul	0882	0920	0845	0891	0872	0929	0903	0917	0852	0923	0944	0897	0837
Aug	0840	0877	0894	0916	0901	0901	0442	0944	0926	0920	0944	0913	0944
Sep	0908	0907	0871	0794	0862	0889	0893	0891	0869	0784	0871	0916	0907
Oct	0917	0900	0844	0923	0906	0881	0916	0902	0873	0892	0910	0871	0912
Nov	0931	0932	0912	0895	0882	0931	0903	0912	0912	0820	0928	0919	0918
Dec	0929	0908	0903	0897	0926	0847	0899	0896	0900	0935	0919	0842	0924

Table 2: Angstrom parameter over Damaturu

Month	2000	2001	2002	2003	2004	2005	2006	2007	2008	2009	2010	2011	2012
Jan	-	0.232	0.102	0.184	0.139	0.132	0.193	0.140	0.077	0.116	0.227	0.148	0.081
Feb	-	0.054	0.159	0.092	0.088	0.099	0.077	0.117	0.060	0.126	0.151	0.117	0.070
Mar	0.114	0.111	-0.004	0.080	0.069	0.041	0.050	0.078	0.079	0.073	0.070	0.121	0.065
Apr	0.123	0.112	0.121	0.094	0.096	0.048	0.094	0.017	0.078	0.055	0.060	0.063	0.063
May	0.137	0.098	0.110	0.115	0.114	0.189	0.116	0.091	0.150	0.101	0.058	0.062	0.084
Jun	0.093	0.177	0.168	0.058	0.113	0.176	0.161	0.191	0.135	0.169	0.129	0.156	0.086
Jul	0.150	0.226	0.112	0.162	0.138	0.264	0.183	0.216	0.118	0.237	-	0.172	0.106
Aug	0.108	0.143	0.168	0.213	0.179	0.179	-0.031	-	0.251	0.227	-	0.205	-
Sep	0.194	0.192	0.137	0.078	0.128	0.160	0.167	0.163	0.135	0.072	0.137	0.213	0.193
Oct	0.216	0.178	0.111	0.235	0.190	0.149	0.214	0.181	0.139	0.164	0.199	0.137	0.204
Nov	0.276	0.278	0.202	0.170	0.150	0.272	0.183	0.204	0.203	0.094	0.258	0.224	0.219
Dec	0.263	0.193	0.183	0.172	0.249	0.114	0.176	0.170	0.178	0.305	0.221	0.110	0.241

Table 3: Radius of particulate-atmospheric aerosols

Month	2000	2001	2002	2003	2004	2005	2006	2007	2008	2009	2010	2011	2012
Jan	-	4.39E-07	6.05E-07	4.89E-07	5.47E-07	7.05E-07	4.79E-07	5.46E-07	6.49E-07	5.81E-07	4.44E-07	5.35E-07	6.41E-07
Feb	-	6.95E-07	5.20E-07	6.21E-07	6.28E-07	7.34E-07	6.48E-07	5.79E-07	6.83E-07	5.66E-07	5.31E-07	5.80E-07	6.62E-07
Mar	5.84E-07	5.90E-07	8.43E-07	6.43E-07	6.64E-07	7.88E-07	7.04E-07	6.47E-07	6.45E-07	6.57E-07	6.62E-07	5.74E-07	6.72E-07
Apr	5.71E-07	5.87E-07	5.73E-07	6.18E-07	6.14E-07	7.81E-07	6.17E-07	7.84E-07	6.47E-07	6.93E-07	6.82E-07	6.77E-07	6.77E-07
May	5.50E-07	6.11E-07	5.91E-07	5.82E-07	5.84E-07	6.58E-07	5.81E-07	6.22E-07	5.32E-07	6.06E-07	6.87E-07	6.78E-07	6.36E-07
Jun	6.19E-07	4.97E-07	5.08E-07	6.86E-07	5.86E-07	6.68E-07	5.18E-07	4.82E-07	5.52E-07	5.08E-07	5.62E-07	5.24E-07	6.31E-07
Jul	5.32E-07	4.44E-07	5.87E-07	5.16E-07	5.49E-07	6.04E-07	4.91E-07	4.54E-07	5.78E-07	4.34E-07	-	5.04E-07	5.98E-07
Aug	5.95E-07	5.41E-07	5.09E-07	4.58E-07	4.95E-07	6.66E-07	9.33E-07	-	4.21E-07	4.43E-07	-	4.66E-07	-
Sep	4.78E-07	4.80E-07	5.50E-07	6.48E-07	5.63E-07	6.81E-07	5.11E-07	5.15E-07	5.53E-07	6.58E-07	5.51E-07	4.58E-07	4.80E-07
Oct	4.55E-07	4.96E-07	5.89E-07	4.35E-07	4.83E-07	6.90E-07	4.57E-07	4.93E-07	5.47E-07	5.14E-07	4.73E-07	5.50E-07	4.67E-07
Nov	3.99E-07	3.98E-07	4.69E-07	5.07E-07	5.32E-07	5.98E-07	4.91E-07	4.68E-07	4.68E-07	6.18E-07	4.14E-07	4.46E-07	4.52E-07
Dec	4.10E-07	4.80E-07	4.91E-07	5.04E-07	4.23E-07	7.20E-07	4.99E-07	5.06E-07	4.96E-07	3.76E-07	4.49E-07	5.91E-07	4.30E-07

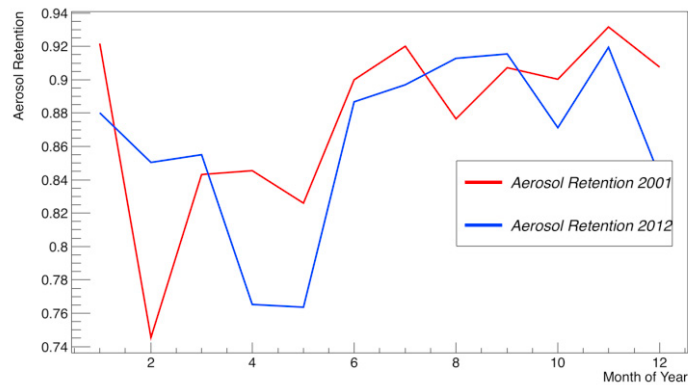


Figure 6: Aerosol Retention

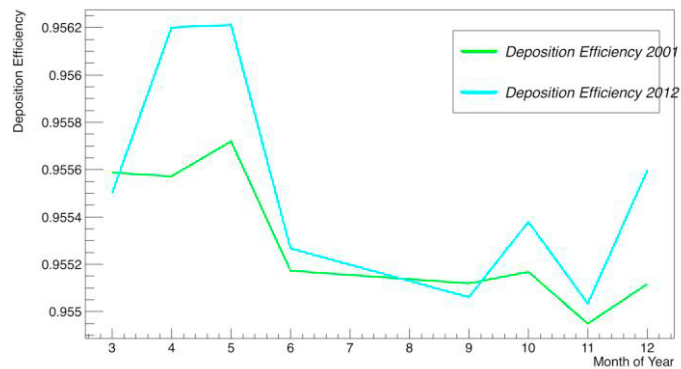


Figure 7: Deposition Efficiency

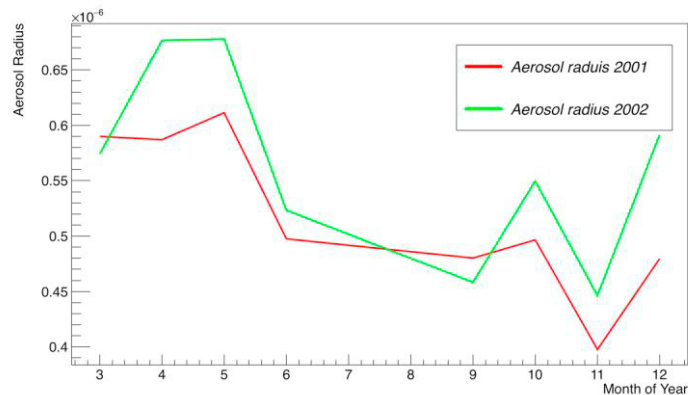


Figure 8: Aerosol Radius

4. Conclusion

The yearly corrosion rate has almost doubled since 2004. Hence, atmospheric corrosion in regions of high aerosol loading is high. Higher accuracy of the modified Faraday model can be achieved using ground dataset.

Acknowledgements

The authors wish to appreciate their institutions. The authors acknowledge NASA for primary dataset.

References

- [1]. Emetere Moses E., Akinyemi M.L. & Oladimeji T.E. (2016) Statistical Examination Of The Aerosols Loading Over Kano, Nigeria: The Satellite Observation Analysis, *Scientific Review Engineering and Environmental Sciences*, 72: 167-176
- [2]. Emetere M.E., Akinyemi M.L., & Akinojo O., (2015) Parametric retrieval model for estimating aerosol size distribution via the AERONET, LAGOS station, *Environmental Pollution*, 207 (C), 381-390
- [3]. Emetere, Moses Eterigho, (2016) Statistical Examination of the Aerosols Loading Over Mubi-Nigeria: The Satellite Observation Analysis, *Geographica Panonica*, 20(1), 42-50
- [4]. Moses Eterigho Emetere, (2017). Investigations on aerosols transport over micro- and macro-scale settings of West Africa, *Environ. Eng. Res.*, 22(1), 75-86
- [5]. M. E. Emetere, (2017). Impacts of recirculation event on aerosol dispersion and rainfall patterns in parts of Nigeria, *GLOBAL NEST JOURNAL* 19 (2), 344-352
- [6]. Rosa Vera, Diana Delgado, Blanca Rosales, *Corros. Sci.* 50 (2008) 1080-1098.
- [7]. Rosa Vera, Patricia Verdugo, Marco Orellana, Eduardo Muñoz, *Corros. Sci.* 52 (2010) 3803-3810
- [8]. H.C. Vasconcelos, B.M. Fernández-Pérez, J. Morales, R.M. Souto, S. González, V. Cano, and J.J. Santana (2014). Development of Mathematical Models to predict the Atmospheric Corrosion Rate of Carbon Steel in Fragmented Subtropical Environments, *Int. J. Electrochem. Sci.*, 9: 6514 -6528
- [9]. A.A. Kokhanovsky, W. Von Hoyningen-Huene, J.P. Burrows, Atmospheric aerosol load as derived from space, *Atmospheric Research*, 81 (2006), pp. 176-185
- [10]. ASTM International, Volume 03.02, Standards G 5, G 48, G 59, G 61, G 102 (ASTM International, 2003: West Conshohocken, PA).